Chapter 5 Analysis of the scalability of a cascaded filled-aperture coherent beam combining system

5.1. Introduction

Coherent beam combining (CBC) has been implemented with both tiled-aperture and filled-aperture schemes. In both schemes, the combining efficiency (the useful combined output optical power divided by the input optical power) is degraded by various noise and loss sources, including the relative phase error between the element beams, the polarization mismatch, the intensity mismatch, the relative element beam pointing error, the absorption and scattering loss of optical components, and a less-than-unity fill factor in the tiled-aperture scheme or non-ideal near-field overlap in the filled-aperture scheme. Influence of the relative phase error and the less-than-unity fill factor on the combining efficiency and beam quality has been studied for the tiled-aperture scheme[52]. Among all the factors, the control of the relative phase between the element beams remains the most critical and difficult task. In the last chapter, we proposed, analyzed, and demonstrated using a full electronic servo system made of multilevel PLLs to address this issue. However, the OPLLs introduce some residual phase error between the element beams, and the VCO loop introduces a non-zero steady state phase error between the element beams. In the presence of these phase errors, a combining efficiency of 94% is achieved when combining two beams in fiber. In this chapter, I will study to what extent these phase errors will affect a CBC system of combining a large number of beams.

The OPLL servo system can be applied to both the tiled-aperture and the filled-aperture schemes. Analysis of the combining efficiency of a tiled-aperture scheme has been given in [52]. Here I focus on analyzing the combining efficiency of the filled-aperture scheme in the presence of various noise sources, particularly the residual phase noise of the OPLLs, the frequency jitter of the VCO and the resulting non-zero

steady state phase error in the VCO loops, the phase front deformation due to the combining beam splitters and mirrors, and the intensity noise. Our analysis will focus on the scalability of the system given all the noise sources. A rigorous analysis should consider the coupling of all the different factors, which is a very difficult task. Here I will assume that they do not affect each other and that one can consider them separately. Since high power fiber amplifiers will be used to boost the optical power, the phase noise introduced by the fiber amplifier will also be discussed and characterized.

5.2 Combining efficiency of the filled-aperture scheme

In a filled-aperture CBC scheme, multiple beams can be combined with a combiner such as a $N \times 1$ fiber coupler. Alternatively two beams are overlapped and combined with a beam splitter. A cascaded binary-tree scheme can then be used to scale the system to combine a large number of beams. Now consider combining N beams at a combiner. The combined intensity at the output of the combiner, averaged over time and space, $\overline{I_p}$, is given by

$$\overline{I_p} = \overline{\left| \sum_i \vec{E}_i \left[r_\perp, \Phi_i \left(r_\perp, t \right) \right] \right|^2} \tag{5.1}$$

where $\vec{E}_i \left[r_\perp, \Phi_i \left(r_\perp, t \right) \right]$ is the complex electric field of the individual beam *i* having a phase fluctuation $\Phi_i \left(r_\perp, t \right)$. $\Phi_i \left(r_\perp, t \right)$ is a function of both time *t* and the transverse coordinate $\vec{r}_\perp$. The $\vec{r}_\perp$ dependence of $\vec{E}_i$ allows for the consideration of wave-front overlap, e.g., alignment mismatch. The temporal and spatial dependence of $\Phi_i \left(r_\perp, t \right)$ allows for the consideration of the degree of mutual coherence and the phase front error between the element beams due to the OPLL residual phase noise, the surface deformation of the optical components, and the pointing error.

Fig. 5.1 shows an example of combining two beams using a beam splitter. Two plane

waves, E_1 and E_2, at the same frequency with fixed relative phase are incident upon a beam splitter having an amplitude reflectivity *r*. At the outputs of the beam splitter there are two pairs of waves propagating at right angles, whose intensities are given by

$$\begin{aligned} I_{P1} &= \alpha\left[E_1^2 r^2 + E_2^2\left(1-r^2\right) + 2E_1E_2r\left(1-r^2\right)^{1/2}\cos\left(\Delta\phi\right)\right] \\ I_{P2} &= \alpha\left[E_2^2 r^2 + E_1^2\left(1-r^2\right) + 2E_1E_2r\left(1-r^2\right)^{1/2}\cos\left(\Delta\phi+\pi\right)\right] \end{aligned} \tag{5.2}$$

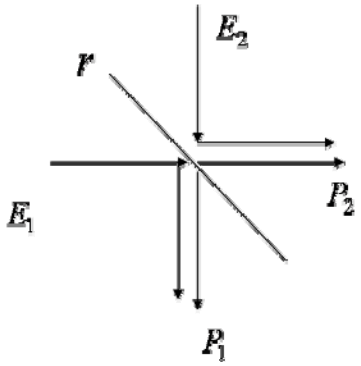

Fig. 5.1 Example of coherent beam combining using a beam splitter. *r* is the reflectivity of the beam splitter.

where $\Delta\phi$ is the phase difference between the two incident waves and α is a constant factor. In the simplest case the two beams possess equal amplitudes, and the beam splitter has a 50:50 splitting ratio, i.e., $r = 1/\sqrt{2}$, $E_1 = E_2 = E_0$. In this case Eq. (5.2) is simplified to

$$I_{P1} = E_0^2\left[1+\cos\left(\Delta\phi\right)\right],\ I_{P2} = E_0^2\left[1-\cos\left(\Delta\phi\right)\right] \tag{5.3}$$

In the ideal case, $\Delta\phi = 0$, all the input power comes out of output 1 and the combining efficiency is 100%. When a position and time dependent phase noise and an intensity variation are present, the combining efficiency becomes

$$\begin{aligned} \eta &= \frac{\overline{I_p}}{\overline{I_1}+\overline{I_2}} = \frac{1}{4}\overline{\left|\sqrt{1+r_1}+\sqrt{1+r_2}\exp\left(i\phi\right)\right|^2} \\ &\approx 1-\frac{1}{4}\overline{\phi^2}-\frac{1}{8}\left(\overline{r_1^2}+\overline{r_2^2}\right) \end{aligned} \tag{5.4}$$

where r_1, r_2 stands for the relative intensity noise (RIN) of beam 1 and 2, and ϕ represents the differential phase error between the two beams. The bar over r_1, r_2, and ϕ stands for the averaging over either time or space depending on the situation. In obtaining Eq. (5.4) I have assumed that the noises have zero mean and are small enough so that the higher order expansion terms can be ignored. To the second-order, the phase noise and the intensity noise are not coupled to each other and hence their effects will be studied separately. Having understood the effect of noises on combining two beams, I will proceed to the analysis of the combination of any number of beams.

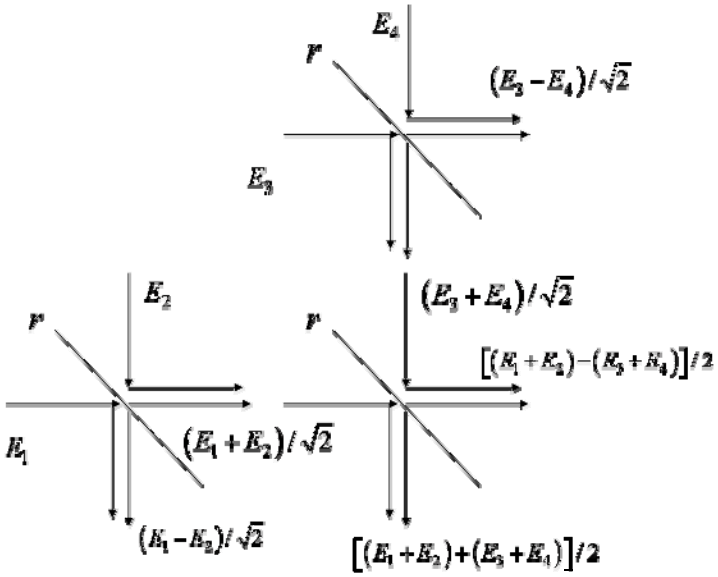

Fig. 5.2 Schematic diagram of a 2-level binary-tree filled-aperture CBC system

5.2.1 Effect of OPLLs residual phase noise

Fig. 5.2 shows a schematic diagram of a 2-level binary-tree filled-aperture CBC system. This scheme can be scaled to an arbitrary number of beams $N = 2^n$ where n is the number of levels in the binary tree structure. Assuming all the beams have equal amplitudes and are perfectly aligned, the combined field takes the form of

$$E_t = E_0 \sum_{i=1}^{N} e^{i\phi_i} \tag{5.5}$$

where $\phi_i(t)$ represents the phase of the individual beam *i* referred to a common reference phase plane. The intensity of the combined field is proportional to the square of the electric field. Normalizing the combined power by the total input power, one obtains the CBC efficiency

$$\eta = \frac{1}{N^2} \overline{\sum_{i,j=1}^{N} e^{i(\phi_i - \phi_j)}} \tag{5.6}$$

I further assume that ϕ_i obeys a Gaussian distribution with zero mean and variance $\overline{\phi_i^2(t)} = \sigma^2$. If ϕ_i and ϕ_j are uncorrelated, then $\overline{\exp\left[i(\phi_i - \phi_j)\right]} = e\left(-\delta_{i,j}\sigma^2\right)$ [52, 63] where $\delta_{i,j}$ is the Kronecker's delta. Eq. (5.6) then becomes

$$\eta = 1 - \frac{N-1}{N}\left(1 - e^{-\sigma^2}\right) \tag{5.7}$$

Assuming $\sigma^2 << 1$, Eq. (5.7) further reduces to

$$\eta = 1 - \frac{(N-1)}{N}\sigma^2 \tag{5.8}$$

As can be seen, the combining efficiency converges to $1-\sigma^2$ for a large number of beams. In Chapter 2 I have obtained the phase noise of the *i*th locked slave laser as

$$\phi_i(s) = \frac{G_{op}}{1+G_{op}}\phi_m^n(s) + \frac{1}{1+G_{op}}\phi_{fr,i}^n(s) \tag{5.9}$$

where ϕ_m^n and $\phi_{fr,i}^n$ are, respectively, the phase noise of the master laser and the *i*th slave laser the under free-running condition, and G_{op} is the open loop transfer function of the *i*th OPLL. If one takes the inverse Fourier transform of Eq. (5.9) and plug it into

$\overline{\phi_i(t)-\phi_j(t)}$ of Eq. (5.6), the first term relating to the phase noise of the master laser ϕ_m^n will cancel out as long as G_{op} is the same for different OPLLs. Thus, one concludes that the phase noise of the master laser does not affect the combining efficiency, since it acts as a common phase reference for all the slave lasers. The second term of Eq. (5.9) is uncorrelated among different slave lasers. If the corresponding variance is σ^2, Eqs. (5.7) and (5.8) can be used to calculate the degraded combining efficiency. In Fig. 5.3 I plot the combining efficiency calculated with the small signal approximation as a function of the rms phase error σ for N=2 and N=8. The small signal approximation agrees well with the Monte Carlo simulation results for small σ.

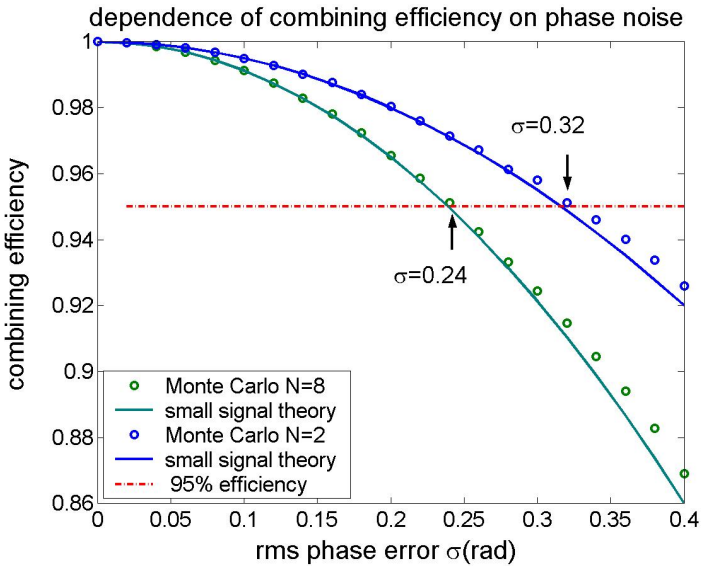

Fig. 5.3 Calculated combining efficiency as a function of the residual differential phase noise

From Eq. (5.8), for a given number of beams and a desired combining efficiency, the rms phase error has to satisfy

$$\sigma \le \sqrt{(1-\eta)\frac{N}{N-1}} \tag{5.10}$$

e.g, if 8 beams are to be combined with an efficiency $\eta = 95\%$, the rms phase error has to be smaller than $0.24rad$. For the IPS OPLL the smallest rms phase error I have measured is around $0.13rad$, which ultimately limits the combining efficiency to ~98%.

5.2.2 Effect of the frequency jitter of the VCO

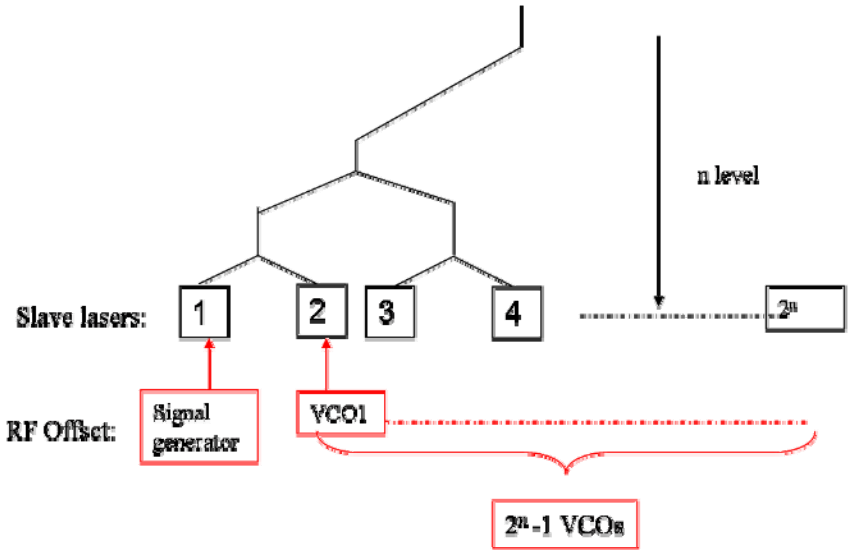

Fig. 5.4 Schematic diagram of a binary-tree filled-aperture CBC system using the VCO loops to correct for the optical path-length variation in fibers

In Chapter 4 I discussed the use of a VCO loop to correct for the optical path-length variation in fibers. I pointed out that a non-zero steady state phase error between the element beams is required to tolerate the frequency jitter of the VCO, and leads to a reduced combining efficiency. In this section I will evaluate the influence of the frequency jitter of the VCO and the nonzero steady-state phase error on the combining efficiency of a cascaded filled-aperture CBC system.

In Chapter 4 I derived that the steady state solution of the phase error in the VCO loop is

$$\phi_{ev,ss} = \cos^{-1}\left(1 - \frac{\omega_{os} - \omega_{v,f}}{K_v}\right) \tag{5.11}$$

where ω_{os} is the frequency of the RF offset signal provided by the signal generator and $\omega_{v,f}$ is the frequency of the free-running VCO, and K_v is the VCO loop gain. Eq. (5.11) has a solution when

$$0 < \left(\omega_{os} - \omega_{v,f}\right) / K_v < 2 \tag{5.12}$$

The combining efficiency is given by $\left(1+\cos\phi_{ev}\right)/2$, therefore one wants to minimize $\phi_{ev,ss}$ to maximize the combining efficiency. However, if the steady state frequency difference $\omega_{os} - \omega_{v,f}$ takes a negative value, Eq. (5.11) has no solution which means the VCO loop will lose lock. Assume that the frequency jitter of the free-running VCO has Gaussian distribution with zero mean and variance σ_ω. Obviously, if $\omega_{os} - \omega_{v,f} = 0$ the VCO could only acquire lock half of the time. If one sets $\omega_{os} - \omega_{v,f}$ equal to $x\sigma_\omega$, where x is a positive number, the quantity $\omega_{os} - \omega_{v,f}$ obeys the Gaussian distribution with mean value $x\sigma_\omega$ and variance σ_ω. The probability for $\left(\omega_{os} - \omega_{v,f}\right)/K_v$ to take a negative value is described by the cumulative distribution function of Gaussian distribution

$$F\left(-x;0,1\right) = \frac{1}{\sqrt{2\pi}} \int_{-\infty}^{-x} \exp\left(-\frac{u^2}{2}\right) du \tag{5.13}$$

If x is small and $\sigma_\omega << K_v$, the probability that $\left(\omega_{os} - \omega_{v,f}\right)/K_v > 2$ is very small and can be ignored. Then the probability that Eq. (5.11) has a solution, or equivalently, that the VCO loop can acquire lock, is given by $1 - F\left(-x;0,1\right)$. E.g, if one lets $\left(\omega_{os} - \omega_{v,f}\right)_{ss} = 2\sigma_\omega$, the probability that the VCO loop is in lock is given by $1 - F\left(-2;0,1\right) = 97.72\%$.

In the binary-tree cascaded filled-aperture scheme, a VCO loop is needed each time two beams are combined. If $N = 2^n$ beams are to be combined, the number of VCO

loops will be $2^n - 1$ (refer to Fig. 5.4). If any one of the VCO loops loses lock, the whole system will be disrupted. To simplify the analysis, I assume that the VCO loops are uncorrelated, so that the probability that all the VCO loops are in lock is given by

$$P_{lock} = \left[1 - F\left(-x; 0, 1\right)\right]^{2^n - 1} \tag{5.14}$$

Meanwhile, the combining efficiency is reduced due to the frequency jitter and the non-zero $\phi_{ev,ss}$ even when the system is in lock. At each combining level of the binary-tree scheme, the combining efficiency is

$$\begin{aligned} \eta &= \left(1 + \overline{\cos\phi_{ev}}\right)/2 \\ &= 1 - \frac{\omega_{os} - \omega_{v,f}}{2K_v} \end{aligned} \tag{5.15}$$

In deriving Eq. (5.15) I have used Eq. (5.11). Assuming $\omega_{os} - \omega_{v,f} = x\sigma_\omega$, the combining efficiency of a locked system with *n* levels is

$$\eta_{lock} = \left(1 - \frac{x\sigma_\omega}{2K_v}\right)^n \tag{5.16}$$

Now one takes into account the fact that the system stays in lock only with a certain probability. Therefore the true combining efficiency should be the product of P_{lock} and η_{lock}

$$\eta = \left[1 - F\left(-x; 0, 1\right)\right]^{2^n - 1} \cdot \left(1 - \frac{x\sigma_\omega}{2K_v}\right)^n \tag{5.17}$$

P_{lock} is a monotonously increasing function of x, while η_{lock} is a monotonously decreasing function of x in the range $0 < x\sigma_\omega / K_v < 2$ where Eq. (5.11) has a solution. Hence an optimal value of x can be chosen to maximize the efficiency described by Eq. (5.17). In Fig. 5.5(a) I plot the combining efficiency as a function of the normalized frequency detuning $x = \left(\omega_{os} - \omega_{v,f}\right)/\sigma_\omega$ for a given normalized frequency jitter $\sigma_\omega / K_v = 0.05$. For each value of *n*, an appropriate value of *x* can be chosen to maximize

the overall combining efficiency.

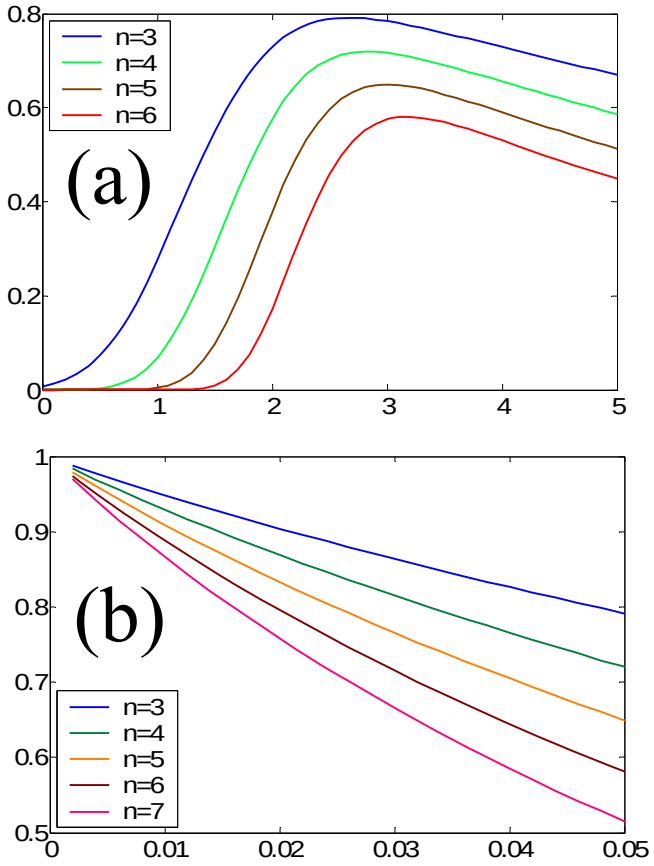

Fig. 5.5 (a) Combining efficiency as a function of the normalized frequency detuning $x = \left(\omega_{os} - \omega_{v,f}\right)/\sigma_{\omega}$ given $\sigma_{\omega}/K_v = 0.05$. A maximum value can be reached by picking the appropriate value of *x*. (b) Maximum combining efficiency as a function of the normalized VCO frequency jitter σ_{ω}/K_v. ω_{os} is the frequency of the RF offset signal provided by the signal generator, $\omega_{v,f}$ is the frequency of the free-running VCO, σ_{ω} is the rms frequency jitter of the VCO, and K_v is the VCO loop gain. The number of element beams is 2^n.

In Fig. 5.5(b) I plot the maximum combining efficiency as a function of the

normalized frequency jitter σ_ω / K_v for different values of *n*. The combining efficiency drops quickly with the increase of both σ_ω / K_v and *n*. To combine a large number of beams, it is therefore critical to have a small value of σ_ω / K_v to achieve a high combining efficiency. In the CBC experiment with one VCO loop presented in Section 4.3.2, I estimate the combining efficiency lost about 2% due to the residual phase error in the OPLLs and 4% due to the non-zero steady state phase error due to the frequency jitter of the VCO. The corresponding value of σ_ω / K_v is about 0.03. As I have pointed out in Section 4.3.2.c, one solution to reduce σ_ω / K_v is to reduce σ_ω, e.g., to use a cleaner VCO with smaller frequency jitter. Another solution is to increase K_v using a lag-lead filter. With such a filter σ_ω / K_v can be reduced by an order of magnitude, and the combining efficiency penalty due to this steady state phase error can be reduced to less than 10% even for n = 7 (128 element beams).

5.2.3 Effect of phase front deformation due to optical components

Optical components such as beam splitters and reflection mirrors used in the combining system introduce phase front deformations in addition to absorption and scattering losses. Though this noise source has nothing to do with the OPLL servo system, I would like to emphasize it here because its influence on the combining efficiency could be more significant than that of the phase error in the OPLLs and the VCO loops I have analyzed.

I use Eqs. (5.6) and (5.7) to calculate the combining efficiency. In this case the bar in Eq. (5.6) represents averaging over space instead of time. Two beams passing through the same beam splitter or reflected by the same mirror will see the same phase front deformation. Thus the phase front deformations of the two beams are correlated. This scenario is illustrated in Fig. 5.6(a). Beam 1 and 2 are combined at beam splitter 1 and

see the same phase front deformation ϕ_1. Beam 3 and 4 see the same phase front deformation ϕ_2, and beam 1,2,3 and 4 also see the same phase front deformation ϕ_3, etc. A second scenario is illustrated in Fig. 5.6(b). This happens, for example, when two beams are combined at a beam splitter, where one beam is transmitted through it and the other one is reflected. Hence the two beams see different phase front deformations.

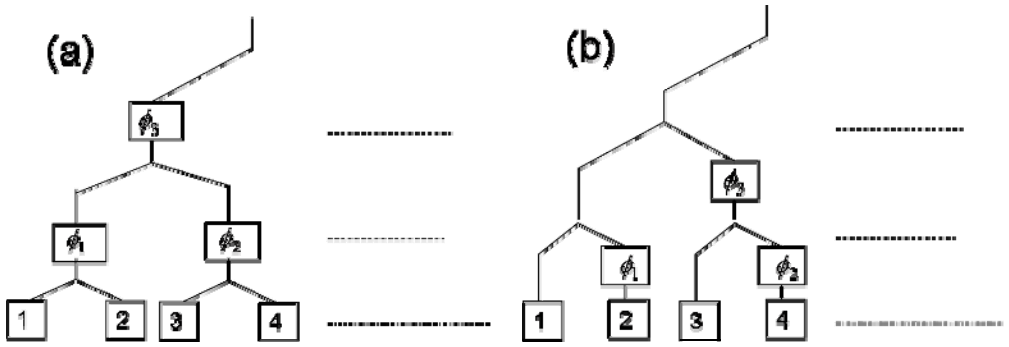

Fig. 5.6 Two scenarios of phase front deformation caused by the combining optics

I first look at scenario 1. The phase front deformations caused by different beam splitters should be uncorrelated and I will assume that the deformations obey Gaussian distribution with zero mean and variance σ^2. One can define a distance function between any two individual laser beams labeled by index *i* and *j*,

$$D(i,j)=\begin{cases}2\left[\log_2|i-j|\right], & i\neq j\\ 0, & i=j\end{cases} \tag{5.18}$$

$D(i,j)$ indicates the number of different beam splitters (or mirrors) which the beams *i* and *j* go through. For example, in Fig. 5.6(a) $D(1,2)=0$ because beam 1 and 2 go through the same beam splitters, and $D(1,3)=2$ because beam 1 and 3 go through two different beam splitters. The combining efficiency can then be calculated as

$$\eta=\frac{1}{N^2}\overline{\sum_{i,j=1}^{N}e^{i(\phi_i-\phi_j)}}=\frac{1}{N^2}\sum_{i,j=1}^{N}e^{-\frac{1}{2}D(i,j)\sigma^2} \tag{5.19}$$

where the total number of beams is $N = 2^n$. An analytical result can be obtained using mathematical recursion if the small error approximation is assumed

$$e^{-\frac{1}{2}D(i,j)\sigma^2} \approx 1-\frac{1}{2}D(i,j)\sigma^2, \quad \frac{1}{2}D(i,j)\sigma^2 << 1 \tag{5.20}$$

Eq. (5.19) then reduces to

$$\eta = \frac{1}{2^{2n}}\left(2^{2n} - \frac{\sigma^2}{2}\sum_{i,j=1}^{2^n} D(i,j)\right) \tag{5.21}$$

If one defines the function $f(n) = \sum_{i,j=1}^{2^n} D(i,j)$, then

$$f(n+1) = \sum_{i,j=1}^{2^{n+1}} D(i,j) = \left(\sum_{i,j=1}^{2^n} + \sum_{i,j=2^n+1}^{2^{n+1}} + \sum_{i=1}^{2^n}\sum_{j=2^n+1}^{2^{n+1}} + \sum_{i=2^n+1}^{2^{n+1}}\sum_{j=1}^{2^n}\right) D(i,j) \tag{5.22}$$

Since $D(i,j)$ only depends on the difference of the indices $|i-j|$, the first two terms in Eq. (5.22) are the same and are equal to $f(n)$. The other two terms are also equal to each other. Therefore Eq. (5.22) becomes

$$\begin{aligned} f(n+1) &= 2f(n) + 2\sum_{i=1}^{2^n}\sum_{j=2^n+1}^{2^{n+1}} 2\left[\log_2|i-j|\right] \\ &= 2f(n) + 2\sum_{i=1}^{2^n}\sum_{j=2^n+1}^{2^{n+1}} 2n \end{aligned} \tag{5.23}$$

Using mathematical recursion one obtains

$$f(n+1) = 2^{n+3}\sum_{i=1}^{n} i2^{i-1} \tag{5.24}$$

Using the mathematical relation

$$\sum_{i=1}^{n} ix^{i-1} = \left(\sum_{i=0}^{n} x^i\right)' = \left(\frac{1-x^{n+1}}{1-x}\right)' = \frac{(nx-n-1)x^n+1}{(x-1)^2} \tag{5.25}$$

and after some algebra one obtains

$$f(n) = (n-2)2^{2n+1} + 2^{n+2} \tag{5.26}$$

Substituting Eq. (5.26) back into Eq. (5.21) gives us the combining efficiency

$$\eta = 1 - \left[(n-2) + 2^{1-n} \right] \sigma^2 \tag{5.27}$$

For the second scenario described in Fig. 5.6(b), calculating the combining efficiency is not so straightforward. However one can make a slight modification of the diagram Fig. 5.6(b) to make it similar to Fig. 5.6(a). Take any triangle in the tree structure of Fig. 5.6(b), one can split the phase front error ϕ in one arm into two uncorrelated phase front errors ϕ_1 and ϕ_2 on both arms and let $\overline{\phi_1^2} = \overline{\phi_2^2} = \frac{1}{2}\overline{\phi^2} = \frac{1}{2}\sigma^2$, as displayed in Fig. 5.7. Next I will prove that Fig. 5.7(a) and Fig. 5.7(b) have equivalent contribution to the combining efficiency calculated using Eq. (5.19).

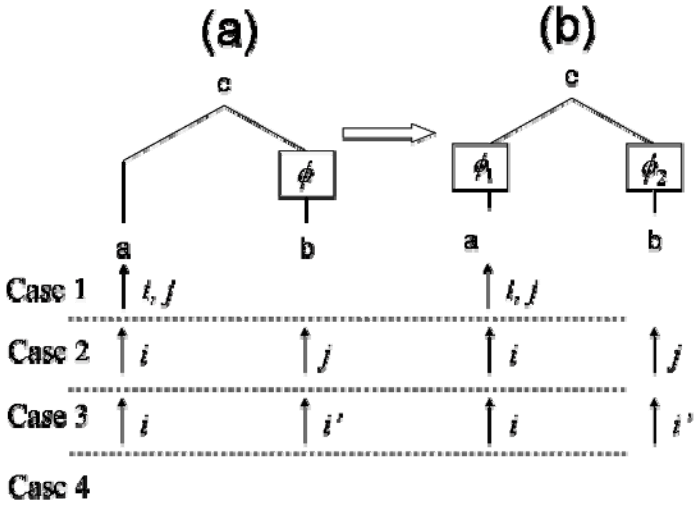

Fig. 5.7. Splitting (a) the one-side phase error into (b) two-side phase errors. Four cases need to be considered to calculate the combining efficiency (Eq. (5.19)). Case 1: both beams *i* and *j* are from the same node a or b. Case 2: one beam is from node a and the other beam is from node b. Case 3: one beam (e.g. *i*) is from this triangle and the other beam is not. *i*' is the image of beam *i* in this triangle. Case 4: neither *i* nor *j* goes through this triangle.

There are four cases that arise while calculating the contribution of this triangle to

any two beams *i* and *j* in Eq. (5.19). In the first case, both the beams *i* and *j* come in through the same node in Fig. 5.7 (either a or b). This triangle adds a common phase front error to the beams *i* and *j*. Therefore both Fig. 5.7(a) and Fig. 5.7(b) have no contribution to the quantity $\overline{\left(\phi_i-\phi_j\right)^2}$ in Eq. (5.19). In the second case, where one beam comes in through node a and the other beam through node b, both triangles in Fig. 5.7(a) and Fig. 5.7(b) contribute the same amount $\overline{\phi_1^2+\phi_2^2}=\overline{\phi^2}$ to $\overline{\left(\phi_i-\phi_j\right)^2}$. The third case happens when one beam (e.g. *i*) goes through either node a or node b, and the other beam (e.g. *j*) does not go through this triangle. In this case one can always find the image beam *i*' of beam *i* going through this triangle. If we calculate the contribution of this triangle to the quantity $\overline{\left(\phi_i-\phi_j\right)^2}+\overline{\left(\phi_{i'}-\phi_j\right)^2}$, Fig. 5.7(a) and Fig. 5.7(b) are the same. The fourth case is when neither beam *i* nor *j* goes through this triangle, and splitting the phase front error does not change anything. Therefore Fig. 5.7(a) and Fig. 5.7(b) are equivalent under the small signal approximation.

With the above modification, scenario 2 (Fig. 5.7(b)) is similar to scenario 1 (Fig. 5.7(a)) and Eq. (5.21) accordingly changes to

$$\eta=\frac{1}{2^{2n}}\left(2^{2n}-\frac{\sigma^2/2}{2}\sum_{i,j=1}^{2^n}D(i,j)\right) \tag{5.28}$$

with

$$D(i,j)=\begin{cases}2\left[\log_2|i-j|+1\right], & i\neq j\\ 0, & i=j\end{cases} \tag{5.29}$$

Using the same mathematical recursion one obtains

$$\sum_{i,j=1}^{2^n}D(i,j)=(n-2)2^{2n+1}+2^{n+2}+2\left(2^n-1\right)2^n=(n-1)2^{2n+1}+2^{n+1} \tag{5.30}$$

and the combining efficiency is

$$\eta=1-\left[\frac{n-1}{2}+2^{-n-1}\right]\sigma^2 \tag{5.31}$$

One can observe from Eqs. (5.27) and (5.31) that the combining efficiency drops linearly with the number of levels in the tree structure n=$\log_2$N. Typical rms phase front deformations of optical components are about $\lambda/40$ [64]. If N = 8 beams are to be combined, the maximum efficiency limited by phase front deformation is about $\eta \sim 97\%$. This efficiency penalty is comparable to that caused by the residual phase noise in OPLLs and the non-zero steady state phase error in the VCO loops. Since it increases linearly with $\log_2$N, optical components of superior surface flatness have to be used if a large number of beams are to be combined.

5.2.4 Effect of intensity noise

The combining efficiency can also be degraded by intensity noise, as indicated in Eq. (5.4). The intensity noise could arise from the relative intensity noise (RIN) of the slave lasers, the fiber amplifiers, or just the amplitude mismatch errors between the element beams. Assume that there is no phase noise and that the amplitude of the *i*th beam takes the form of $E_i = E_0(1+r_i)$, where r_i is the relative amplitude fluctuation with zero mean and variance $\overline{r_i^2} = \delta^2$. The efficiency of combining N beams affected by the intensity noise can then be calculated as

$$\eta = \overline{I_p} / \sum_{i=1}^{N} \overline{I_i} \approx 1 - \frac{1}{N}\left(1 - \frac{1}{N}\right)\sum_{i=1}^{N} \overline{r_i^2} \tag{5.32}$$

If all the beams have similar intensity fluctuations, the combining efficiency converges to $\eta = 1 - \delta^2$ for a large number N and the efficiency penalty does not increase with the number of beams.

The free-running RIN of state-of-the-art SCLs is typically very small. I have

characterized the RIN of the IPS lasers used in CBC by detecting the power with a photodetector and measuring the output on an oscilloscope. The bandwidth of the photodetector is 12GHz and the bandwidth of the oscilloscope is 500MHz. The measured rms RIN is 2e-4, which is limited by the shot noise and photodetector electronic noise. Since the rms residual phase noise in the OPLLs is about 0.12rad, in Eq.(5.4) the third term is much smaller than the second term and can thus be ignored safely.

Additional intensity noise can also be introduced by the OPLL feedback current. Since the current feedback is used to control the relative phase error between the slave laser and the master laser, the intensity of the slave laser can also be modulated and the magnitude needs to be carefully checked.

Here I only want to estimate the magnitude of the intensity noise caused by the feedback current. Assuming that the FM responses of the circuit and the laser are flat, the current fed back into the SCL is

$$i = i_0 \sin \phi_e \tag{5.33}$$

where ϕ_e is the detected phase difference between the master laser and the slave laser, and i_0 is a constant deciding the loop gain. Assume the intensity modulation responsivity is K_{AM}, the intensity modulation is $\Delta P = K_{AM} i_0 \sin \phi_e$ and the RIN is

$$r_s = \Delta P / P_0 = \frac{K_{AM}}{P_0} i_0 \sin \phi_e \tag{5.34}$$

where P_0 is the DC optical power. K_{AM} can be estimated from the slope of the P-I curve of the slave laser, i.e.,

$$K_{AM} = P_0 / \left(I - I_{th} \right) \tag{5.35}$$

where I_{th} is the threshold current. In Eq. (5.33) i_0 determines the holding range of the OPLL and can thus be calculated by

$$i_0 = \Delta f_h / K_{FM} \tag{5.36}$$

where Δf_h is the holding range and K_{FM} is the FM responsivity of the SCL. Substituting Eqs. (5.35) and (5.36) in Eq. (5.34) one obtains the RIN

$$r_s(t) = \frac{\Delta f_h}{(I - I_{th}) K_{FM}} \sin \phi_e(t) \tag{5.37}$$

Using the typical parameters of the IPS laser OPLL $\Delta f_h \approx 200MHz$, $I - I_{th} \approx 300mA$, $K_{FM} \approx 200MHz/mA$, Eq. (5.37) gives $r_s(t) = \frac{1}{300} \sin \phi_e(t)$. Thus the RIN introduced by the feedback current is at least two orders of magnitude smaller than the residual phase noise of the OPLL, and its effect on the combining efficiency can be neglected.

5.2.5 Effect of fiber amplifier phase noise

SCLs have relatively low output power. To achieve high average power, tens of thousands of SCLs need to be combined, which is very difficult to do. State-of-the-art fiber lasers or fiber amplifiers can emit single frequency beams of hundreds of watts with diffraction limited beam quality. An alternative option to obtain high average power is to use the locked slave laser to seed tens of high power fiber amplifiers, whose output beams are then coherently combined. Since CBC is very sensitive to phase noise, the phase noise introduced by the fiber amplifiers needs to be examined.

Historically there have been two different models proposed to explain the effects of fiber amplifier phase noise. The first model assumes that the amplified spontaneous emission (ASE) in the fiber amplifier adds a multiplicative phase term to the electrical field at the output of the optical amplifier[65, 66], i.e.,

$$E_{out}(t) = \sqrt{G} E_0 e^{i\phi(t)} . e^{i\omega t} . e^{i\phi_a(t)} \tag{5.38}$$

where E_0 is the amplitude of the signal at the amplifier input，G is the optical gain of the amplifier，$\phi(t)$ is the phase of the input signal, and $\phi_a(t)$ is the phase noise

introduced by the amplifier.

This multiplicative phase noise model predicts a linewidth broadening of the signal. Following the derivation in [66], one arrives at an expression for the linewidth broadening due to ASE in the fiber amplifier:

$$\delta\nu = \sqrt{\frac{n_{sp}^2 h\nu.\Delta\nu_s^3\left(G-1\right)^2}{4\pi G P_{in}}} \tag{5.39}$$

where n_{sp}~1 is the spontaneous emission factor, $\Delta\nu_s$ is the input signal linewidth, ν is the optical frequency, and P_{in} is the power of the input signal.

It was further pointed out in [66] that if the effect of ASE is taken into account only over the fiber amplifier bandwidth B_0, the predicted linewidth broadening is much smaller, given by

$$\delta\nu = \frac{n_{sp} h\nu B_0\left(G-1\right)}{4\pi G P_{in}} B_0 \tag{5.40}$$

However, more recent investigations into fiber amplifier phase noise have revealed that this multiplicative model may not be accurate[67, 68]. Instead, an additive noise model has been proposed, where the output field is given by

$$E_{out}(t) = \sqrt{G}E_0 e^{i\phi(t)}.e^{i\omega t} + E_n.e^{i\omega t}.e^{i\phi_a(t)} \tag{5.41}$$

where E_n is the amplitude of the ASE noise within the signal bandwidth. The signal-to-noise ratio of an unsaturated fiber amplifier is given by [39]

$$\left(\frac{S}{N}\right)_{output} = \frac{P_{in}}{\mu h\nu\,\Delta\nu_s}\frac{G}{G-1} \tag{5.42}$$

where μ is the population inversion factor ($\mu \approx 1$).

Since the predicted linewidth broadening (Eq. (5.39) or (5.40)) of the first model can be much smaller than the signal linewidth, a self-heterodyne balanced interferometer experiment as shown in Fig. 5.8(a) is usually employed to measure the linewidth broadening. This measurement removes the phase noise of the laser source, and is therefore more sensitive[68]. In this measurement, when the fiber amplifier is turned off,

one should see a delta function as shown in Fig. 5.8(b). When the amplifier is on, if the phase noise is multiplicative, one expects to see a Lorenzian lineshape as given in Fig. 5.8(c). If the phase noise is additive, one expects to see a delta function with a Lorenzian pedestal, whose width is determined by the sum of the laser and amplifier phase noise. The ratio of the signal power to the noise power (area under the Lorenzian pedestal) is given by Eq. (5.42).

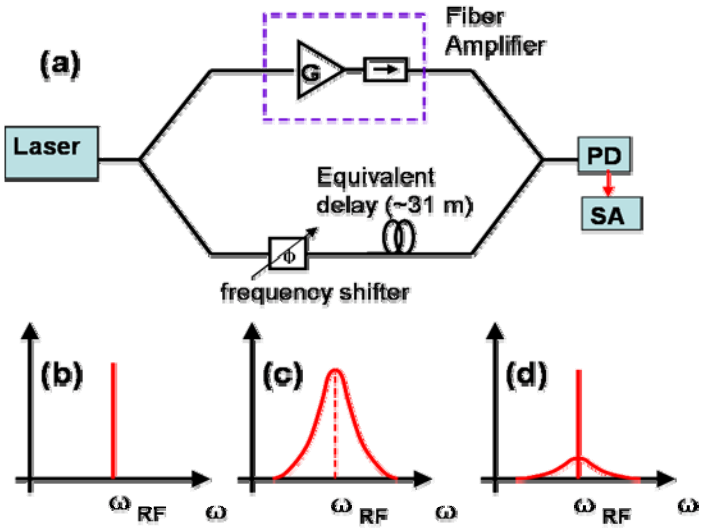

SA: Spectrum analyzer, PD: photodetector

Fig. 5.8 (a) Self-heterodyne fiber amplifier phase noise measurement setup. (b)-(d) Predicted beat spectra with (b) no amplifier noise, (c) multiplicative phase noise, and (d) additive phase noise

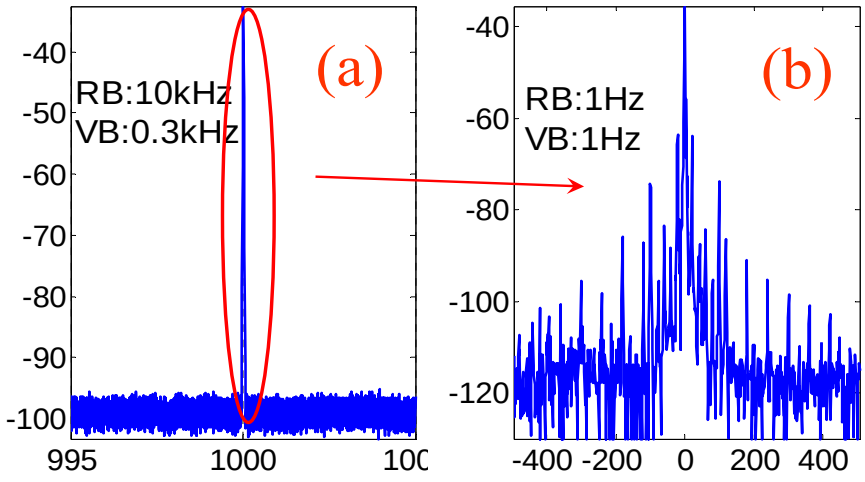

Fig. 5.9 Experimental results of the self-heterodyne fiber amplifier phase noise

measurement with span of (a) 10MHz and (b) 1kHz

I conducted a self-heterodyne balanced interferometer experiment as shown in Fig. 5.8(a). A 1064 nm IPS external cavity SCL is used to seed a Nufern 3 W Yb-doped fiber amplifier. A phase modulator is used as the frequency shifter. In Fig. 5.9, I plot the measured spectrum with a span of 10 MHz and 1kHz. I see neither any observable linewidth broadening down to the resolution limit of the spectrum analyzer (~ 1 Hz) nor a noise pedestal down to the noise floor (67 dB below the signal level). However Fig. 5.9(b) shows the presence of many noise peaks, which are mainly the harmonics of the power line frequency (60 Hz) and are more than 20dB lower than the signal. This noise results from the acoustic noise picked up by the fiber. I replaced the amplifier with a passive fiber of equivalent length (~30m) and observed the same noise peaks.

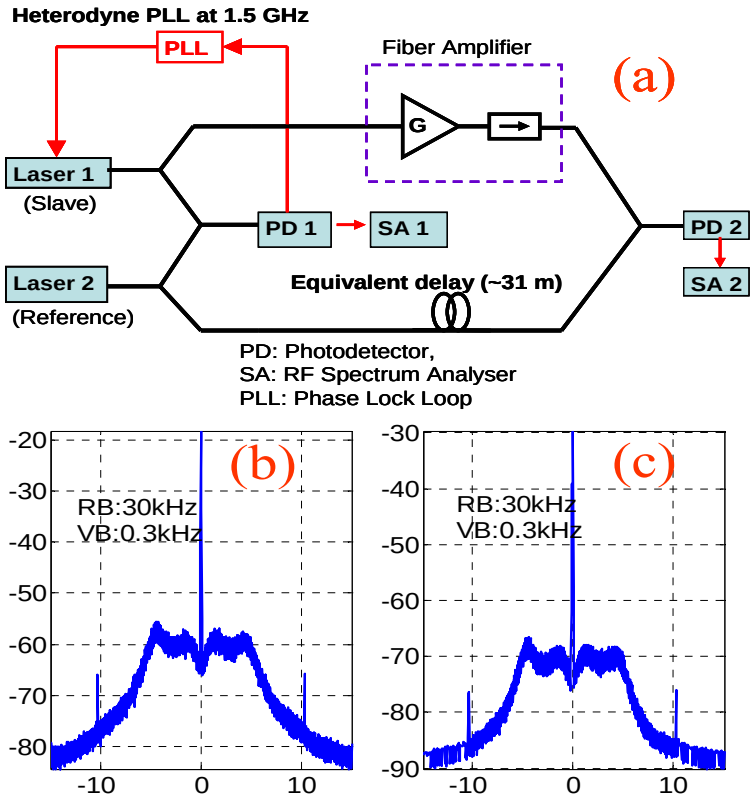

Fig. 5.10 (a) Experimental setup to measure the fiber amplifier phase noise added to the OPLL. (b) and (c) Beat spectra at the photodetectors PD1 and PD2 in (a).

I also performed a direct measurement of the amplifier phase noise added to the OPLL as shown in Fig. 5.10(a). The slave laser is phase locked to the master laser with a frequency offset ω_{os}, amplified and then beat with the master laser in a balanced interferometer to remove the effect of the master laser phase noise. Comparing Fig. 5.10(b) to Fig. 5.10(c), I do not see any effect of phase noise added by the amplifier. In fact, the multiplicative phase noise model[66] predicts a linewidth broadening of less than 1Hz for an laser linewidth of 500 kHz, fiber amplifier gain of 40, and an input power level of 75 mW in our case. The additive phase noise model predicts a signal-to-noise ratio[39] of ~120 dB. In either case, the effect of ASE in the fiber amplifier is far below our measurement sensitivity and can be safely neglected compared to the other factors reducing the combining efficiency. While the amplifier does introduce a lot of thermal phase variation [25] and picks up acoustic noise, these variations are at very low frequency compared to the VCO loop bandwidth of ~100kHz discussed in chapter 4 and should be significantly suppressed by the VCO loops.

5.3 Conclusion

In Chapters 4 and 5, I have presented a detailed study using OPLLs to coherently combine optical beams. The full electronic servo system enabled by the OPLLs technology eliminates the need for optical phase shifters and should significantly reduce the cost and size of the system. In the preliminary experiment of combining two laser beams, a promising combining efficiency of 94% is achieved. This approach can be applied to both tiled-aperture and filled-aperture CBC implementations. In either case, the efficiency penalty due to the residual phase noise of the OPLLs is less than 2% if IPS external cavity lasers are used. In the filled-aperture approach, the efficiency penalty caused by the phase error in the VCO loops and the phase front deformation scales up as $\sim\log_2 N$. This poses a serious challenge if a large number of beams are to be combined.

Fortunately, with the power of single-mode fiber amplifiers reaching hundreds of watts and even kilowatts, combining tens of beams can scale the power up to the regime of 10kW or even 100kW.